materials

MDPI

Article

Pentafluorophenyl Platinum(II) Complexes of PTA and its N-Allyl and N-Benzyl Derivatives: Synthesis, Characterization and Biological Activity

Paolo Sgarbossa [1,*], Urszula Śliwińska-Hill [2], M. Fátima C. Guedes da Silva [3], Barbara Bażanów [4], Aleksandra Pawlak [5], Natalia Jackulak [4], Dominik Poradowski [6], Armando J. L. Pombeiro [3] and Piotr Smoleński [7,*]

[1] Dipartimento di Ingegneria Industriale and CIRCC, Consorzio Interuniversitario per le Reattività Chimiche e la Catalisi, Università di Padova, via Marzolo 9, 35131 Padova, Italy
[2] Department of Analytical Chemistry, Faculty of Pharmacy, Wrocław Medical University, Borowska 211 A, 50-566 Wrocław, Poland; urszula.sliwinska-hill@umed.wroc.pl
[3] Centro de Química Estrutural, Instituto Superior Técnico, Universidade de Lisboa, Av. Rovisco Pais, 1049-001 Lisboa, Portugal; fatima.guedes@tecnico.ulisboa.pt (M.F.C.G.d.S.); pombeiro@tecnico.ulisboa.pt (A.J.L.P.)
[4] Department of Veterinary Microbiology, Wrocław University of Environmental and Life Sciences, Norwida 31, 50-375 Wrocław, Poland; barbara.bazanow@upwr.edu.pl (B.B.); natalia.jackulak@upwr.edu.pl (N.J.)
[5] Department of Biochemistry, Pharmacology and Toxicology, Wrocław University of Environmental and Life Sciences, Norwida 31, 50-375 Wrocław, Poland; aleksandra.pawlak@upwr.edu.pl
[6] Department of Biostructure and Animal Physiology, Wrocław University of Environmental and Life Sciences, Kożuchowska 1/3, 51-631 Wrocław, Poland; dominik.poradowski@upwr.edu.pl
[7] Faculty of Chemistry, University of Wroclaw, F. Joliot-Curie 14, 50-383 Wrocław, Poland
* Correspondence: paolo.sgarbossa@unipd.it (P.S.); piotr.smolenski@chem.uni.wroc.pl (P.S.)

Received: 10 October 2019; Accepted: 22 November 2019; Published: 26 November 2019

Abstract: From the well-known 1,3,5-triaza-phosphaadamantane (PTA, **1a**), the novel N-allyl and N-benzyl tetrafuoroborate salts 1-allyl-1-azonia-3,5-diaza-7-phosphaadamantane (APTA(BF_4), **1b**) and 1-benzyl-1-azonia-3,5-diaza-7-phosphaadamantane (BzPTA(BF_4), **1c**) were obtained. These phosphines were then allowed to react with (Pt(μ-Cl)(C_6F_5)(tht))$_2$ (tht = tetrahydrothiophene) affording the water soluble Pt(II) complexes *trans*-(PtCl(C_6F_5)(PTA)$_2$) (**2a**) and its bis-cationic congeners *trans*-(PtCl(C_6F_5)(APTA)$_2$)(BF_4)$_2$ (**2b**) and *trans*-(PtCl(C_6F_5)(BzPTA)$_2$)(BF_4)$_2$ (**2c**). The compounds were fully characterized by multinuclear NMR, ESI-MS, elemental analysis and (for **2a**) also by single crystal X-ray diffraction, which proved the *trans* configuration of the phosphine ligands. Furthermore, in order to evaluate the cytotoxic activities of all complexes the normal human dermal fibroblast (NHDF) cell culture were used. The antineoplastic activity of the investigated compounds was checked against the human lung carcinoma (A549), epithelioid cervix carcinoma (HeLa) and breast adenocarcinoma (MCF-7) cell cultures. Interactions between the complexes and human serum albumin (HSA) using fluorescence spectroscopy and circular dichroism spectroscopy (CD) were also investigated.

Keywords: platinum(II) pentafluorophenyl complexes; N-alkylated PTA; biological activity; HSA interactions

1. Introduction

The water-solubility of 1,3,5-triaza-7-phosphaadamantane (PTA), its diverse mode of coordination, ease of functionalization and modification have made this compound a ligand of choice in coordination chemistry [1–3], catalysis [4–12] and bioinorganic chemistry [13,14]. N-Functionalization is the simplest modification of PTA; it leaves the cage structure and the P-coordinating ability intact and affords a series of cationic species with tunable properties in terms of hydrophilicity and reactivity. For these reasons, this scope has been addressed in the last decade by synthesizing derivatives bearing alkyl (methyl [15–17], ethyl and propyl [18–20], butyl [21] or hexadecyl [22]), benzyl [23–25] or pyridyl [26] groups.

Since the development of new metallodrugs for cancer treatment based on tertiary phosphines/aminophosphines [27–32] the interest for these types of ligands has reemerged. Both PTA and its derivatives have been applied in the synthesis of biologically active Pt(II/IV) [33–37], Au(I) [38–40], Ru(II) [41–47], Ag(I) [48–51] and Cu(I) [52–55] metal complexes. Indeed, phosphines can provide beneficial properties such as better stability in biological media (thus reducing undesired side reactions) and moldable affinity for polar and apolar environments in the cell (modifying the compounds transport across the membrane and their accumulation). Moreover, the choice of cationic N-functionalized PTA ligands can in principle increase the interaction with the polyanionic DNA strands [56].

An approach to circumvent cross-resistance is to change the functionality on the metal center namely by decreasing the number of available coordination sites. Monofunctional complexes can be active [57–60] and have the advantage of having ancillary ligands, which, as such, modify sterically and electronically the behavior of the resulting complex.

Recently Moreno et al. have successfully used the pentafluorophenyl group as a stabilizing ancillary ligand toward platinum for biological applications [61,62]. The C_6F_5 ligand has higher *trans*-effect than amines in labilizing the Pt–Cl bond [63] and the ability to increase the Lewis acidity of platinum [64–67] while modifying the hydro/lipophilicity of the complex.

Spectroscopic studies involving transition metal complexes and blood proteins such as the human serum albumin (HSA) are essential for the understanding of the biological activity of the drugs in terms of nature and strength of the interactions [68,69]. Protein–drug interactions are responsible for the distribution of the drug in the body and affect the chemotherapy effectivity and toxicity [70]. The standard example, cisplatin reaches 50–61% human serum albumin fixation after intravenous administration [71,72]. This binding is considered to be practically irreversible because only less than 5% of the drug is released from the system [73].

Platinum(II) complexes with *trans* geometry have proved to be interesting candidates to replace the commonly used cisplatin in view of its known adverse effects (mainly its toxicity) and to overcome acquired resistance (due to DME, drug-metabolizing enzymes or genetic variation) [74–77]. Trans-bisphosphino Pt(II) complexes have shown antiproliferative activity, being able to generate reactive oxygen species, targeting both mitochondria and genomic DNA [78], but also showed affinity toward protein models comparable or higher than cisplatin [79].

In our attempt to contribute to the knowledge of phosphine *trans*-platinum compounds and their biological activity, we synthesized the PTA (**1a**) N-allyl and N-benzyl tetrafuoroborate derivatives 1-allyl-1-azonia-3,5-diaza-7-phosphaadamantane (APTA(BF_4), **1b**) and 1-benzyl-1-azonia-3,5-diaza-7-phosphaadamantane (BzPTA(BF_4), **1c**) and the water soluble Pt(II) hexafluorophenyl complexes *trans*-(PtCl(C_6F_5)(PTA)$_2$) (**2a**), *trans*-(PtCl(C_6F_5)(APTA)$_2$)(BF_4)$_2$ (**2b**) and *trans*-(PtCl(C_6F_5)(BzPTA)$_2$)(BF_4)$_2$ (**2c**; Figure 1).

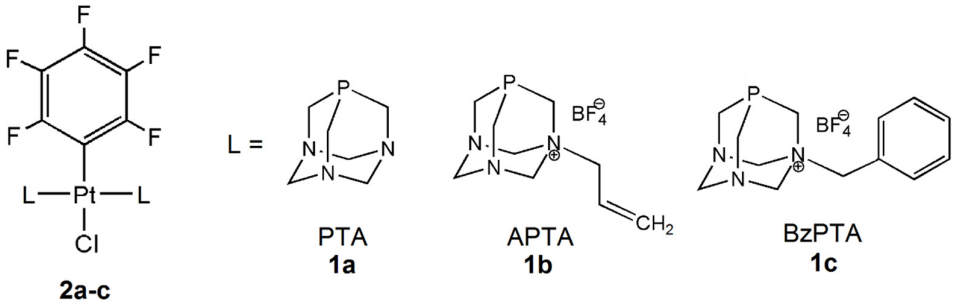

Figure 1. New PTA-based pentafluorophenyl Pt(II) complexes **2a–c**.

All the new compounds have been fully characterized and the Pt(II) complexes were evaluated with NHDF (normal human dermal fibroblasts), A549 (human lung carcinoma), HeLa (human epithelioid cervix carcinoma) and MCF7 (human breast adenocarcinoma) cell cultures. NHDF cell line was used only as a control. Cancer cell lines were chosen based on cisplatin utilization in their standard treatment protocols. In addition, the interactions between the platinum complexes and HSA were investigated by circular dichroism (CD) and fluorescence spectroscopy. The association constants, acting forces and protein's secondary structure changes are discussed based on the obtained results.

2. Experimental

2.1. General

^{1}H, $^{13}C\{^{1}H\}$, $^{31}P\{^{1}H\}$ and ^{19}F NMR spectra at 298 K were run on a Bruker AC200 spectrometer operating at 200.13, 50.323, 81.015 and 188.25 MHz, respectively; δ values (ppm) are reported relative to $SiMe_4$, 85% H_3PO_4, and $CFCl_3$ as reference. ESI-MS analyses were performed using LCQ-Duo (Thermo-Finnigan) operating in the positive ion mode. Instrumental parameters: capillary voltage 10 V, spray voltage 4.5 kV; capillary temperature 200 °C; mass scan ranged from 150 to 2000 m/z; N_2 was used as sheath gas and the He pressure inside the trap was kept constant. The pressure directly read by an ion gauge (in the absence of the N_2 stream) was 1.33×10^{-5} Torr. Sample solutions were prepared by dissolving the compounds in acetonitrile. Sample solutions were directly infused into the ESI source by a syringe pump at 8 μL/min flow rate. Elemental analyses were performed by the Microanalysis Laboratory of the Department of Chemical Sciences of the University of Padova.

2.2. Materials and Methods

All synthetic steps were carried out under dinitrogen atmosphere using standard Schlenck techniques. Solvents were dried and purified according to standard methods [80].

$(Pt(C_6F_5)(\mu\text{-}Cl)(tht))_2$ [81,82], PTA [15] and BzPTA(Cl) [23] were synthesized following procedures reported in the literature.

2.3. Cell Cultures

NHDF (normal human dermal fibroblasts; PromoCell, C-12302), A549 (human lung carcinoma; ATCC, No CCL-185 ™), HeLa (human cervix carcinoma; ATCC, No CCL-2 ™) and MCF7 (human breast adenocarcinoma; ATCC, No HTB-22 ™) were used. NHDF, A549, HeLa and MCF7 cell lines were cultured in DMEM (Lonza, Basel, Switzerland). Media were supplemented with 10% FBS (Biological Industries, Kibbutz Beit-Haemek, Israel), 4 mM L-glutamine (Biological Industries, Kibbutz Beit-Haemek, Israel), 100 U/mL of penicillin and 100 μg/mL of streptomycin (Sigma, Steinheim, North Rhine-Westphalia, Germany).

2.4. Cell Viability Assays

All cell cultures were inserted in a 96-well plate (Eppendorf, Freie und Hansestadt Hamburg, Germany) in a concentration of 10^5 cells per well.

Compounds **2a–c** and ligands **1a–c** were dissolved in distilled water and diluted to afford concentrations of 30, 3, 0.3 and 0.03 μg/mL in DMEM and incubated in standard conditions for 72 h, after which the MTT (Sigma, Steinheim, North Rhine-Westphalia, Germany) assay was carried out. 20 μL of MTT (5 mg/mL) was added to each well, incubation for 4 h at 37 °C was implemented, and then 80 μL of lysis buffer was added. The test consists in the enzymatic reduction of the tetrazolium salt MTT in metabolically active cells. The metabolite, purple-colored formazan is measured colorimetrically, using a multiwell plate reader. The optical density (OD) was measured using a spectrophotometric microplate reader (Multiscan Go, Thermo Fisher, Waltham, MA, USA) at 570 nm with reference wavelength of 630 nm. The viability of the investigated cell cultures was estimated using following formula: viability% = (average OD for test group/average OD for control group) × 100. The untreated cells were used as a control group.

2.5. Cytotoxic Assay-Quantitative Suspension Test According to EN 14476

NHDF, A549, HeLa and MCF7 cells at a density of 4×10^4 cells/mL were incubated in 96-well polystyrene plate (NUNC, Roskilde, Zealand, Denmark) for 24 h. Substances were tested using EN 14476 [83]. Product test solutions were prepared in 10% DMSO and DMEM supplemented with additional 10% FBS and L-glutamine. Solutions of the complexes **2a–c** and pro-ligands at concentrations from 300 μg/mL to 3×10^{-9} μg/mL were prepared and transferred (100 μL) into cell culture units containing 100 μL of cells suspension. Eight units were inoculated with each dilution. Plates were incubated in 37 °C/5% CO_2 and observed daily for up to 4 days for the development of cytotoxic effects, using an inverted microscope (Olympus Corp., Hamburg, Germany; Axio Observer, Carl Zeiss, MicroImaging GmbH, Baden-Württemberg, Germany).

2.6. Octanol–Water Partition Coefficient Determination

The log(P) values corresponding to the octanol–water partition coefficient was adjusted to the solubility properties of the compounds [84]. Complexes were dissolved in water previously saturated with octanol, to achieve concentrations of 10^{-3} M. At 24 °C, 25 mL of octanol saturated with water was introduced into a 100 mL flask equipped and then 25 mL of the aqueous complex solutions was added. The two-phase mixture thus obtained was stirred vigorously for 20 min. After separation of the phases and removal of the respective solvents under vacuum, the attained residues were weighed. Values for log(P) of −0.11, −0.71 and −0.40 for **2a**, **2b** and **2c**, respectively, were obtained.

2.7. HSA Interaction

High purity free-HSA (>96%, Sigma-Aldrich, Steinheim, North Rhine-Westphalia, Germany) was used as purchased. The stock solutions of platinum complexes (200 μM) were freshly prepared in double distilled water prior to their use. The HSA solutions (200 μM) were prepared in PBS (pH 7.40). In the final step, the samples contained (protein):(drug) equal 1:0–1:9 in PBS, where C_{HSA} was 10 μM. Measurements were done after 24 h incubation at 300, 305 and 310 K. HSA concentration was determined, using A_{279} (1 mg/mL) as 0.531 [85].

2.7.1. Fluorescence Measurements

Emission fluorescence spectra were recorded using Hitachi F-2700 spectrofluorimeter (Tokio, Japan) in 1.0 cm quartz cells in the 300–400nm range. Trp-214 fluorescence of HSA was measured at 295 nm. The intensity at 335 nm (Trp-214) was used to achieve the quenching mechanism and calculate the binding constants and thermodynamic parameters according to literature reports.

2.7.2. CD Measurement

Circular dichroism spectra were recorded on a Jasco J-715 spectropolarimeter, over the range of 190–250 nm in 0.1 cm cuvettes. The α-helical content of HSA was calculated from the molar ellipticity (θ) at 208–210 nm using Equations (1) and (2) [86]:

$$MRE_{209} = \frac{Observed_{CD}\,(mdeg)}{C_p \cdot n \cdot l \cdot 10}, \quad (1)$$

$$\alpha - helix\ (\%) = \frac{MRE_{209} - 4000}{33000 - 4000} \times 100, \quad (2)$$

where *MRE* is the mean residue ellipticity, C_p is the molar concentration of the protein, n is the number of amino acid residues (583) and l is the path-length (0.1 cm).

2.8. Synthesis and Analytical Data

APTA(BF_4) **1b.** Of PTA (6.36 mmol) 1.00 g was dissolved in 50 mL of anhydrous acetone at room temperature and treated under stirring with 0.59 mL of allyl iodide (1.08 g, 6.45 mmol). After 1 h reflux, the volume of the solution was taken to ca. 10 mL and added with 15 mL of diethyl ether to give a white precipitate. The solid was filtered, dried under vacuum and dissolved in 50 mL of anhydrous methanol. After adding 1.88 g of $TlBF_4$ (6.45 mmol), the clear solution was left stirring at room temperature for 30 min. The precipitate of TlI was filtered off and the solution was concentrated on a rotary evaporator. The product was obtained by precipitation with diethyl ether, subsequently washed three times with 5 mL of Et_2O, recrystallized from methanol, and dried under vacuum. Yield 1.51 g, 83.3%. Anal. Calc. for $C_9H_{17}BF_4N_3P$: C, 37.92; H, 6.01; N, 14.74%; Found: C, 37.77; H, 5.98; N, 14.68%. ^{1}H NMR (δ, D_2O): 5.99–5.78 (m, 1H, C*H*CH$_2$N$^+$); 5.68–5.54 (m, 2H, C*H*$_2$CH); 4.80 (dd, $^1J_{HH}$ = 12 Hz, 4H, N$^+$C*H*$_2$N); 4.41 (dd, $^1J_{HH}$ = 14 Hz, 2H, NC*H*$_2$N); 4.20 (d, $^2J_{PH}$ = 14 Hz, 2H, N$^+$C*H*$_2$P); 3.87–3.66 (m, 4H, NC*H*$_2$P); 3.47 (d, $^1J_{HH}$ = 8 Hz, 2H, CHC*H*$_2$N$^+$); ^{13}C{^{1}H} NMR (δ, D_2O): 130.5 (*C*HCH$_2$N$^+$); 122.5 (*C*H$_2$CH); 79.1 (N$^+$CH$_2$N); 70.0 (NCH$_2$N); 65.7 (CHCH$_2$N$^+$); 53.7 (d, $^1J_{PC}$ = 33 Hz, N$^+$CH$_2$P); 46.2 (d, $^1J_{PC}$ = 21 Hz, NCH$_2$P); ^{31}P{^{1}H} NMR (δ, D_2O): −82.8 (s); ^{19}F{^{1}H} NMR (δ, D_2O): −150.4 (BF_4). ESI-MS (CH_3OH): *m*/*z* 198.05 (100%) [M − BF_4]$^+$.

BzPTA(BF_4) **1c.** Of BzPTA(Cl) (0.70 mmol) 0.20 g was dissolved in 50 mL of anhydrous methanol at room temperature and added with 0.20 g (0.70 mmol) of $TlBF_4$. After stirring for 1 h the precipitate of TlCl was filtered off and the solution was concentrated on a rotary evaporator. The solid product obtained by precipitation with diethyl ether was washed three times with 5 mL of Et_2O, recrystallized from methanol, and dried under vacuum. Yield 0.24 g, 96.0%. Anal. Calc. for $C_{13}H_{19}BF_4N_3P$: C, 46.60; H, 5.72; N, 12.54%; Found: C, 46.87; H, 5.68; N, 12.18%. ^{1}H NMR (δ, D_2O): 7.50–7.40 (m, 5H, Ar); 4.79 (dd, $^1J_{HH}$ = 14 Hz, 4H, N$^+$C*H*$_2$N); 4.33 (dd, 2H, $^1J_{HH}$ = 14 Hz, NC*H*$_2$N); 4.16 (d, $^2J_{PH}$ = 6 Hz, 2H, N$^+$C*H*$_2$P); 4.07 (s, 2H, PhC*H*$_2$N$^+$); 3.92–3.59 (m, 4H, NC*H*$_2$P); ^{13}C{^{1}H} NMR (δ, D_2O): 132.9, 130.9, 129.3, 124.5 (Ph); 78.7 (N$^+$CH$_2$N); 69.4 (NCH$_2$N); 66.8 (PhCH$_2$N$^+$); 52.8 (d, $^1J_{PC}$ = 33 Hz, N$^+$CH$_2$P); 45.6 (d, $^1J_{PC}$ = 21 Hz, NCH$_2$P); ^{31}P{^{1}H} NMR (δ, D_2O): −82.85 (s); ^{19}F{^{1}H} NMR (δ, D_2O): −150.4 (BF_4). ESI-MS (CH_3OH): *m*/*z* 248.06 (100%) [M − BF_4]$^+$.

(PtCl(C_6F_5)(PTA)$_2$) **2a.** Of (Pt(μ-Cl)(C_6F_5)(tht))$_2$ (0.21 mmol) 0.20 g were dissolved in 30 mL of anhydrous dichloromethane at room temperature and treated with 0.13 g of PTA (0.83 mmol). After stirring for 1 h, the solution was concentrated on rotary evaporator and treated with diethyl ether. The solid precipitated as a white powder was filtered on a Gooch funnel, washed three times with 5 mL of Et_2O, and dried under vacuum. **2a** is soluble in DMSO and dichloromethane, sparingly soluble in H_2O ($S_{25\,°C} \approx 0.35$ mg mL^{-1}), MeOH and EtOH and insoluble in diethyl ether, C_6H_6 and alkanes. Yield 0.28 g, 99%. Anal. Calc. for $C_{18}H_{24}ClF_5N_6P_2Pt$: C, 30.37; H, 3.40; N, 11.81%; Found: C, 30.58; H, 5.48; N, 11.61%. ^{1}H NMR (δ, CD_2Cl_2): 4.47 (m, 12H, PC*H*$_2$N); 4.09 (s, 12H, NC*H*$_2$N); ^{13}C{^{1}H} NMR (δ, CD_2Cl_2): 73.1 (s, NCH$_2$N); 49.7 (m, NCH$_2$P); ^{31}P{^{1}H} NMR (δ, CD_2Cl_2): −61.8 (s, $^1J_{Pt\text{-}P}$ = 2453 Hz). ^{19}F{^{1}H} NMR (δ, CD_2Cl_2): −118.3 (m, *o*-F, $^3J_{Pt\text{-}F}$ = 435 Hz, $^3J_{F\text{-}F}$ = 14.1 Hz), −160.5 (m, *p*-F, $^3J_{F\text{-}F}$ = 14.1 Hz), −162.3 (m, m-F). ESI-MS (CH_3OH): *m*/*z* 713.08 (100%) [M + H]$^+$. Crystals suitable for X-Ray analysis were obtained by slow growth through diffusion of Et_2O in a solution of **2a** in CH_2Cl_2.

(PtCl(C_6F_5)(APTA)$_2$)(BF_4)$_2$ **2b.** Through a synthetic procedure similar to the one described for complex **2a**, complex **2b** was obtained from 0.05 g of (Pt(μ-Cl)(C_6F_5)(tht))$_2$ (0.05 mmol) dissolved in 10

mL of methanol and treated with 0.06 g of APTA(BF_4) (0.21 mmol). **2b** is soluble in DMSO, dichloromethane and H_2O ($S_{25°C} \approx 4.0$ mg mL^{-1}), sparingly soluble in MeOH and EtOH and insoluble in diethyl ether, C_6H_6 and alkanes. Yield 0.078 g, 79%. Anal. Calc. for $C_{24}H_{34}B_2ClF_{13}N_6P_2Pt$: C, 29.79; H, 3.54; N, 8.69%; Found: C, 30.03; H, 3.68; N, 8.21%. ^{1}H NMR (δ, DMSO-d_6): 6.04–5.87 (m, 2H, C*H*CH_2N^+); 5.71–5.54 (m, 4H, CH_2CH); 4.99 (dd, 8H, N^+CH_2N); 4.43 (dd, 4H, NCH_2N); 4.36 (s, 4H, N^+CH_2P); 4.02 (dd, 8H, NCH_2P); 3.68 (d, $^3J_{HH}$ = 6 Hz, 4H, $CHCH_2N^+$); ^{13}C{^{1}H} NMR (δ, DMSO-d_6): 128.9 ($CHCH_2N^+$); 124.2 (CH_2CH); 78.8 (N^+CH_2N); 68.7 (NCH_2N); 63.8 ($CHCH_2N^+$); 49.75 (m, N^+CH_2P); 45.3 (m, NCH_2P); ^{31}P{^{1}H} NMR (δ, DMSO-d_6): −41.42 (s, $^1J_{Pt-P}$ = 2628 Hz). ^{19}F{^{1}H} NMR (δ, DMSO-d_6): −117.2 (m, *o*-F, $^3J_{Pt-F}$ = 395 Hz, $^3J_{F-F}$ = 22.6), −148.1 (BF_4), −159.5 (t, *p*-F, $^3J_{F-F}$ = 22.6 Hz), −161.1 (m, *m*-F). ESI-MS (CH_3OH): *m*/*z* 880.05 (100%) $[M - BF_4]^+$.

($PtCl(C_6F_5)(BzPTA)_2)(BF_4)_2$ **2c.** Through a synthetic procedure similar to the one described for complex **2a**, complex **2c** was obtained from 0.05 g of $(Pt(\mu\text{-}Cl)(C_6F_5)(tht))_2$ (0.05 mmol) in 10 mL of methanol and 0.07 g of BzPTA(BF_4) (0.21 mmol). **2c** is soluble in DMSO, dichloromethane and H_2O ($S_{25°C} \approx 3.0$ mg mL^{-1}), sparingly soluble in MeOH and EtOH and insoluble in diethyl ether, C_6H_6 and alkanes. Yield 0.085 g, 77%. Anal. Calc. for $C_{32}H_{38}B_2ClF_{13}N_6P_2Pt$: C, 36.00; H, 3.59; N, 7.87%; Found: C, 36.12; H, 3.51; N, 7.80%. ^{1}H NMR (δ, DMSO-d_6): 7.60–7.36 (m, 10H, Ar); 5.03 (dd, 8H, N^+CH_2N); 4.44 (dd, 4H, NCH_2N); 4.22 (s, 4H, $PhCH_2N^+$); 4.15 (s, 4H, N^+CH_2P); 4.03 (m, 8H, NCH_2P); ^{13}C{^{1}H} NMR (δ, DMSO-d_6): 133.3, 131.0, 129.5, 125.7 (Ph); 79.0 (N^+CH_2N); 68.9 (NCH_2N); 64.7 ($PhCH_2N^+$); 49.1 (m, N^+CH_2P); 45.3 (m, NCH_2P); ^{31}P{^{1}H} NMR (δ, DMSO-d_6): −40.8 (s, $^1J_{Pt-P}$ = 2627 Hz). ^{19}F{^{1}H} NMR (δ, DMSO-d_6): −117.3 (m, *o*-F, $^3J_{Pt-F}$ = 393 Hz, $^3J_{F-F}$ = 22.6), −148.2 (BF_4), −159.5 (t, *p*-F, $^3J_{F-F}$ = 22.6 Hz), −161.1 (m, *m*-F). ESI-MS (CH_3OH): *m*/*z* 980.10 (100%) $[M - BF_4]^+$.

2.9. X-Ray Crystallography

An X-ray quality crystal of **2a** was immersed in cryo-oil, mounted in a Nylon loop and measured at 153 K. Intensity data was collected using a Bruker AXS-KAPPA APEX II diffractometer with graphite monochromatic Mo-Kα (λ = 0.71073) radiation. Data were collected using phi and omega scans of 0.5° per frame and a full sphere of data were obtained. Cell parameters were retrieved using Bruker SMART software and refined using Bruker SAINT [87] on all the observed reflections. Absorption corrections were applied using SADABS [88]. Structures were solved by direct methods by using SIR97 [89] and refined with SHELXL-2014/7 [90]. Calculations were performed using the WinGX System (Version 2014.1) [91]. The hydrogen atoms attached to the methylene carbons were inserted in calculated positions, their Uiso (H) defined as 1.2 Ueq of the parent carbon atoms. Least square refinements with anisotropic thermal motion parameters for all the non-hydrogen atoms and isotropic for most of the remaining atoms were employed. The molecular structure of **2a** in represented in Figure 1, crystallographic details are listed in Table 1 and selected bond distances and angles in the legend of Figure 1. CCDC 1572427 contains the supplementary crystallographic data for this paper. These data can be obtained free of charge from The Cambridge Crystallographic Data Centre via www.ccdc.cam.ac.uk/data_request/cif.

Crystal data for **2a**: $C_{18}H_{24}ClF_5N_6P_2Pt$, M = 711.91, T = 153(2) K, monoclinic, space group $C2/c$, a = 19.9537(17) Å, b = 12.2786(9) Å, c = 10.2981(9) Å, β = 115.314(5)°, V = 2280.8(3) Å^3, Z = 4, Dc = 2.073 g/cm^3, μ = 6.471 mm^{-1}, 10377 reflections collected, 1928 unique, $I > 2\sigma(I)$ (R_{int} = 0.0383), R_1 = 0.0183, $wR2$ = 0.0427, GOF 1.043. CCDC 1572427.

3. Results and Discussion

3.1. Synthesis and Characterization

1,3,5-triaza-7-phosphaadamantane (PTA, **1a**) was allowed to react with allyl iodide and benzyl chloride [8a] in acetone under reflux to give the iodide salt of 1-allyl-1-azonia-3,5-diaza-7-phosphaadamantane (APTA(I)) and benzyl derivative 1-benzyl-1-azonia-3,5-diaza-7-phosphaadamantane (BzPTA(Cl)) in high yields, respectively. The exchange of the halide counterions by tetrafluoroborate on both the latter derivatives afforded the pro-ligands APTA(BF_4) (**1b**) and BzPTA(BF_4) (**1c**) as white and air-stable solids (Scheme 1). The presence of the BF_4 anion proved to

increase the stability to the N-alkylated PTAs and its non-coordinating property was fundamental for the preparation of the platinum(II) complexes.

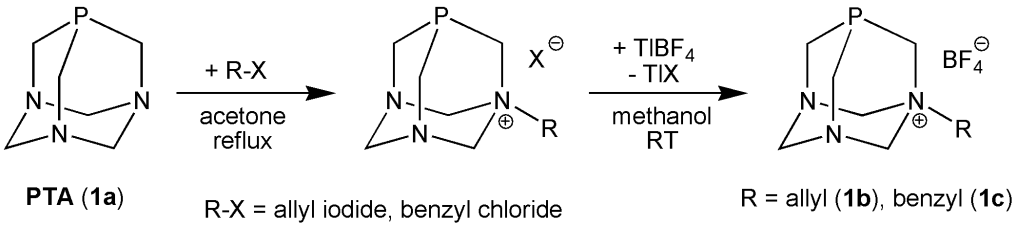

Scheme 1. Synthesis of allyl (**1b**) and benzyl (**1c**) PTA derivatives**.**

^{1}H NMR spectra of **1b** and **1c** (see the Experimental Section) show the typical signals of N-monosubstituted PTA: (i) two AB resonances around 4.8 and 4.4–4.3 ppm for the protons in the lower rim revealing their diastereotopic nature; (ii) a doublet at 4.2 ppm and a ABX-type multiplet at 3.5–3.9 ppm for the protons in the upper rim, enlightening the coupling to phosphorus and (iii) the expected signals for the allyl and benzyl group [4c]. The ^{13}C{^{1}H} NMR spectra are characterized by the expected six singlets of the unsymmetrical alkylated PTA cage in the range 45–70 ppm and, in both cases, the singlet due to the methylene group at around 79 ppm. The signals of the sp^{2} C in the allyl group (2 peaks) of **1b** and the benzylic phenyl ring (5 peaks) of **1c** are in the range 122–133 ppm. The signal for the substituted phenyl C has not been detected.

The ^{31}P{^{1}H} NMR spectra show a single peak at about −83 ppm for both derivatives, which is upfield from the resonance reported for PTA (−98.5 ppm) [92] and very similar to those reported for other N-substituted PTA compounds [15–26].

The platinum pentafluorophenyl complexes *trans*-(PtCl(C_6F_5)(PTA)$_2$) (**2a**) and the bis-cationic *trans*-(PtCl(C_6F_5)(APTA)$_2$)(BF_4)$_2$ (**2b**) and *trans*-(PtCl(C_6F_5)(BzPTA)$_2$)(BF_4)$_2$ (**2c**) have been obtained as white powders with yields in the range 77–99% by reaction of 4 equivalents of **1a**, **1b** or **1c** with the binuclear complex *trans*-(Pt(μ-Cl)(C_6F_5)(tht))$_2$ (tht = tetrahydrothiophene; Scheme 2).

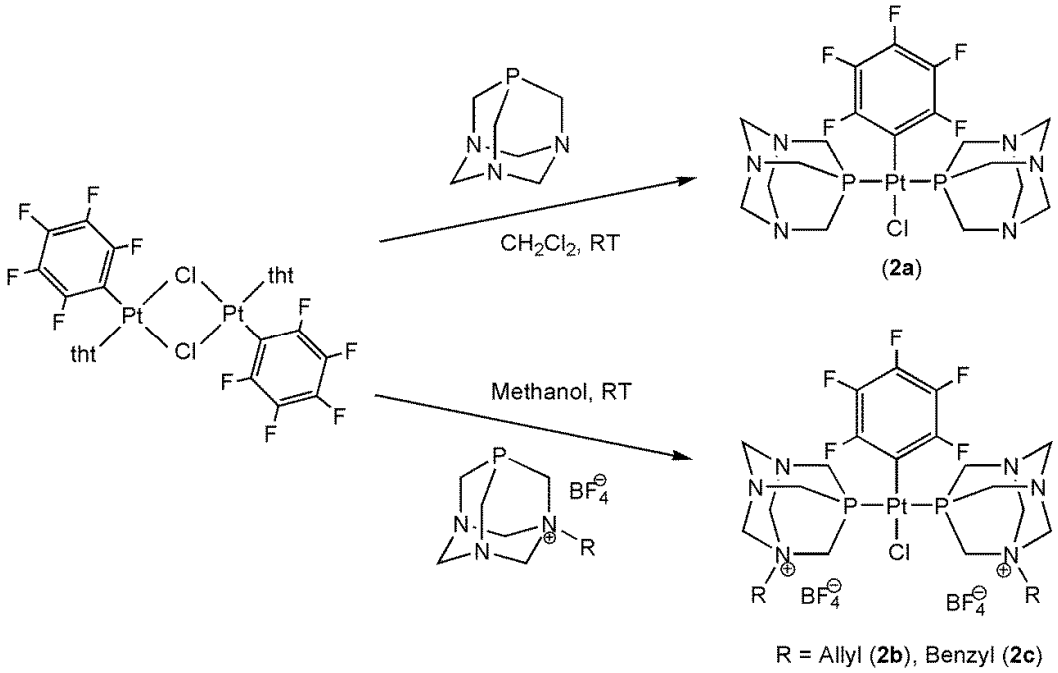

Scheme 2. Synthesis of the pentafluorophenyl Pt(II) complexes **2a–c.**

Complex **2a** is sparingly soluble in water but well soluble in DMSO and other polar solvents and in medium polarity solvents such as dichloromethane. Compounds **2b–c** show a similar behavior but with higher solubility in water due to their cationic nature.

The novel compounds **2a–c** were characterized by elemental analysis, as well as by ^{1}H (Figures S1–S5), ^{31}P{^{1}H}, ^{13}C{^{1}H} and ^{19}F{^{1}H} NMR spectroscopies (see the Experimental Section). The ^{1}H NMR spectra confirm the presence of the phosphines: their resonances are shifted downfield by the electron withdrawing influence of the metal center, and the $^{2}J_{PH}$ coupling constants present lower values. The ^{31}P{^{1}H} NMR spectra show a singlet, as expected for equivalent nuclei in a *trans* geometry. The presence of the phosphine in the Pt(II) complexes is confirmed by the downfield shift, $\Delta\delta$, of the ^{31}P resonance upon coordination: 36.7 (**2a**), 41.4 (**2b**) and 42.1 ppm (**2c**). The P-Pt coupling constants are of 2450 Hz for **2a** and ca. 2628 Hz for **2b** and **2c**. In complex **2a**'s ^{13}C{^{1}H} NMR spectrum, the signals for the upper rim (49.67 ppm) and for the lower rim (73.11 ppm) carbons can be seen, while those of complexes **2b–c** show the typical structure for alkylated PTA cages with peaks in the range 45–69 ppm. In both cases the singlet of the methylene group is around 79 ppm, as for the pro-ligands (see above). Similarly, the signals of the olefinic carbons (2 peaks) in the APTA^{+} moiety of **2b** and the benzylic phenyl ring (5 peaks) of BzPTA^{+} in **2c** are in the range 124–135 ppm. No resonances for the pentafluorophenyl carbons have been detected. However, the presence of this group was confirmed by the ^{19}F{^{1}H} NMR spectra where the $^{3}J_{Pt\text{-}F}$ coupling of the *o*-F nuclei with the ^{195}Pt metal center assume values in the range 440–390 Hz. The ESI-MS spectra of the pro-ligands and the complexes were performed in methanol and confirm the expected formulations.

X-ray quality crystals of complex **2a** (Figure 2) have been obtained by slow diffusion of diethyl ether on a dichloromethane solution of the compound in air and at room temperature. It crystalized in the monoclinic space group *C*2/c, its asymmetric unit including a PTA phosphine ligand and half of the fluorinated moiety. Resulting from the two-fold axis that runs across the molecule, a mononuclear compound is thus constructed from a Pt(II) cation, which is bound to a chloride anion, P-bound to two PTA phosphines and C-bound to one pentafluorobenzene anion, therefore giving rise to a square planar geometry (τ_4 = 0.03) [93]. The pentafluorophenyl ring lies perpendicular to the plan constructed by the Pt-, P- and Cl-atoms (89.8°). The bond lengths involving the metal and the donor atoms (see Figure 1, legend), are within those found in other Pt(II) compounds [94–99]. No classical H-bond interactions could be found in **2a**, but the shortest C–H···N interactions (Figure 1) expand the structure to the third dimension.

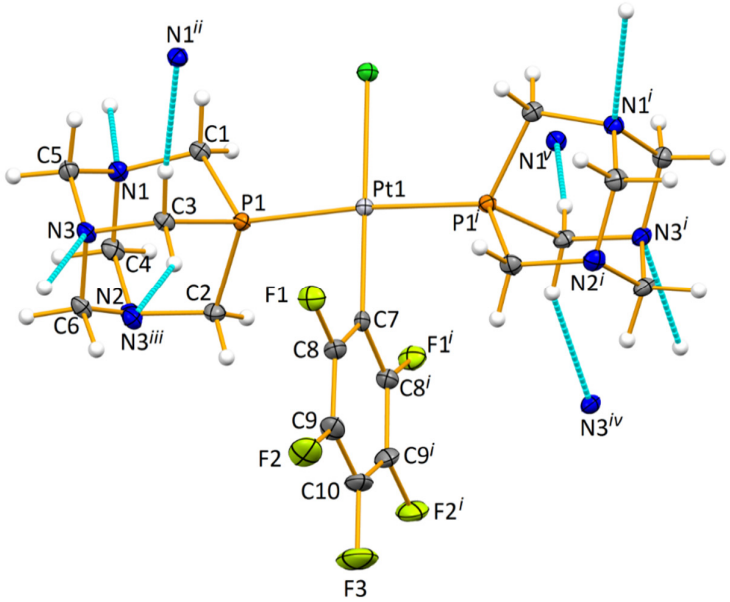

Figure 2. Molecular structure of complex **2a** with a partial atom labeling scheme. Ellipsoids are drawn at 30% probability level. Selected distances (Å) and angles (°): Pt–P1 2.2788(8), Pt–Cl1 2.3688(12), Pt–

C7 2.016(4); P1–Pt1–P1^{i} 175.15(4), P1–Pt1–Cl1 92.43(2), C7–Pt1–Cl1 180.0 and C7–Pt1–P1 87.57(2). Relevant non-classical hydrogen bond interactions C–H···N (represented in dashed light blue color; *d*(C···N) in Å, ∠(C–H···N) in °): C3–H3A···N3 3.465(4), 144 and C3–H3B···N1 3.440(4), 172. Symmetry codes to generate equivalent atoms: (i) 1 − x, y, 1.5 − z; (ii) x, −y, ½ + z; (iii) 1.5 − x, ½ − y, 2 − z; (iv) −1/2 + x, ½ − y, −1/2 + z and (v) 1 − x, −y, 1 − z.

Table 1. Crystal data and structure refinement details for **2a**.

Formula unit	**$C_{18}H_{24}ClF_5N_6P_2Pt$**
Formula weight	711.91
Crystal system	Monoclinic
Space group	*C*2/c
a (Å)	19.9537(17)
b (Å)	12.2786(9)
c (Å)	10.2981(9)
β (°)	115.314(5)
Z	4
Volume (Å^3)	2280.8(3)
T (K)	153(2)
D_c (g cm^{-3})	2.073
μ (mm^{-1})	6.471
θ_{max}, θ_{min} (°)	25.349, 2.589
Rfls. total, unique, observed	10377, 2082, 1928
R_{int}	0.0383
R_1 *,wR_2 # ($I > 2\sigma(I)$)	0.0183, 0.0427
R_1, wR_2 (all data)	0.0214, 0.0440
GOF	1.043

* $R1 = \Sigma||F_o| - |F_c||/\Sigma|F_o|$. # $wR2 = [\Sigma[w(F_o^2 - F_c^2)^2]/\Sigma[w(F_o^2)^2]]^{1/2}$.

3.2. Biologic Assays

Cancer cell lines used in this study belong to one type of neoplasms, derived from epithelial. Those carcinomas hardly respond for treatment and have high potential for metastasis. The fibroblast cell line reflects a normal cell of body. Cytotoxic Assay-Quantitative Suspension Test According to EN 14476 was done as a preliminary investigation. The results were similar to those obtained in MTT test. Considering that MTT method is more detailed, analysis and discussion were carried out on the basis of these results. The IC50 (half maximal inhibitory concentration) values, after 72 h of incubation with the tested compounds, are shown in Table 2.

Table 2. Half maximal inhibitory concentration (IC50) values (μM) of the tested complexes (**2a–c**), pro-ligands (**1a–c**), and cisplatin.

Entry	**Cell line**	**2a**	**2b**	**2c**	**1a [100]**	**1b**	**1c**	**Cisplatin [100]**
1	NHDF	26.07 ± 0.68	26.91 ± 3.5	11.16 ± 3.1	nd[a]	>263.13 ± 13	>223.82 ± 5.7	16.65 ± 2.1
2	A549	15.41 ± 5.3	7.79 ± 1.7	>28.10 ± 1.9	nd[a]	>263.13 ± 0.42	>223.82 ± 23	33.30 ± 4.2
3	HeLa	>42.14 ± 5.5	29.48 ± 1.3	8.89 ± 4.1	nd[a]	65.78 ± 6.6	55.96 ± 16	16.65 ± 3.1
4	MCF7	>42.14 ± 7.9	>31.00 ± 11	>28.10 ± 7.3	nd[a]	>263.13 ± 7.5	72.40 ± 2.4	33.30 ± 4.2

[a] nd = not detectable.

From Table 2, we can see that all three complexes show cytotoxicity against the fibroblasts cell line (NHDF). Compound **2a** and **2b** shows higher cytotoxicity to A549 and lower to HeLa and MCF7

cell lines, while compound **2c** proved more active against HeLa cell lines. All three complexes show cytotoxicity against fibroblasts cell line (NHDF), but lower when compared to A549 or HeLa cell lines. The lower cytotoxicity effect of cisplatin on A549 cell line can be caused by different growing conditions, medium supplementation and exposition time. Cisplatin displayed, in contrast to tested compounds, weaker activity against the chosen neoplastic cell lines (especially A549); comparable doses of cisplatin are toxic for both normal and neoplastic (HeLa) cell lines. It is also worth mentioning that the solubility and stability of compounds **2a–c** in aqua-media were higher than those of cisplatin. Hydrolytic stability tests of **2a–c**, performed at 2.0 mM concentration in NaCl solution (5 or 100 mM in D_2O-d_6/DMSO 10/1) by ^{1}H and ^{31}P NMR spectroscopy, shows no free phosphine after 72 h at room temperature and only partial hydrolysis of the Pt–Cl bond. The bioactivities of **2a–c** coincided with values of their logarithm of 1-octanol/water partition coefficient (log(P), see Experimental). This method is one of the most widely used ones to describe hydrophobic/hydrophilic properties of chemicals. For the accurate biological activity and bioavailability of potential drugs, a balanced solubility in both water and nonpolar compounds such as lipids is required [54]. Indeed, the different activity of the platinum complexes **2a–c** could be related to their more balanced log(P) values, in contrast to cisplatin with strongly negative log(P) factor (−2.21) [101]. The lower cytotoxicity of the new compounds for normal cells in comparison to cancer cells was their undoubted advantage. Even if their cytotoxicity for cancer cells was not radically lower than cisplatin, they could be a reasonable alternative, especially useful in cisplatin resistant therapies. Their good solubility in aqueous solutions is also important, which will allow us to "relieve" therapy with toxic solvents. Further research is thus needed to proof usefulness of the tested compounds in tumor therapy.

3.3. HSA Interactions

The effect of compounds **2b** and **2c** on the fluorescence intensity of HSA (max 335 nm) is shown in Figure 3. It decreased with increasing amounts of the complexes, indicating that some interactions between the two components were taking place. The variation in intensity results from a quenching effect of the metal compounds. In addition, a maximum blue shift of ca. 3 (with **2b**) and 5 (with **2c**) nm was observed, indicating that Trp-214 was placed in a more hydrophobic environment and was less exposed to the solvent. It also suggests that the interaction might occur via the hydrophobic region of the protein [102,103].

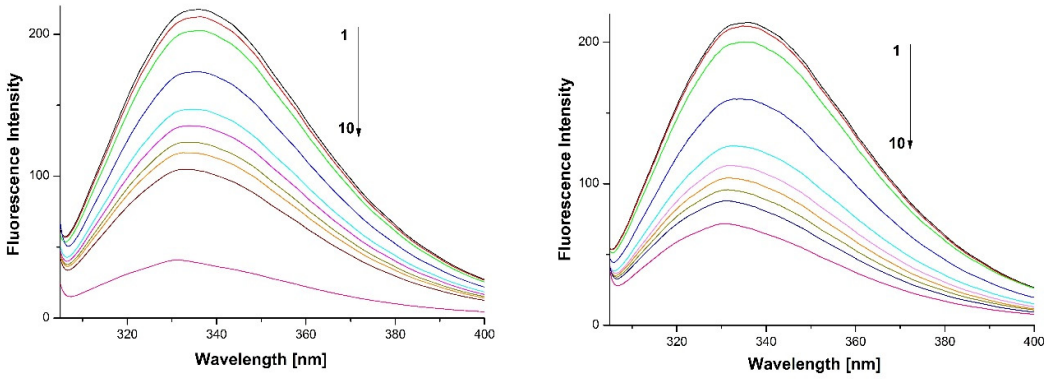

Figure 3. Fluorescence emission spectra of HSA-**2b** (left) and -**2c** (right) systems. Experimental conditions: (1) HSA (10 μM) and (2)–(10) HSA 10 μM with Pt complex at 5, 10, 30, 50, 60, 70, 80, 90 and 100 μM; pH = 7.40, 0.05 M phosphate buffer, incubation at 37 °C during 24 h, λ_{ex} = 295 nm.

The Stern−Volmer plots of HSA in the presence of the platinum compounds as quenchers, at different conditions, are shown in Figure S6 (Equations S1–S2). The calculated Stern-Volmer constants (K_{SV}) and quenching rate constants (Kq) for the interactions between HSA and complexes **2b** and **2c** are listed in Table 3. The obtained results showed that Ksv increased with the increase in temperature, thus indicating that the fluorescence quenching mechanism of HSA by the Pt

compounds was a dynamic one. The maximum expected value of Kq for dynamic processes is 2×10^{10} $M^{-1} \cdot s^{-1}$ [103,104], but the higher value obtained in our study, ca. 10^{12} $M^{-1} \cdot s^{-1}$, shows that specific drug–protein interactions were involved, making Kq larger [105]. It suggests that the fluorescence quenching processes of the HSA-Pt complex systems were initiated by a combined process of dynamic and static quenching.

Fluorescence quenching data were also analyzed to obtain various binding parameters for the interaction of the platinum complexes with HSA, as shown in Figure S7. The association constants (K_A) for complexes **2b** and **2c** and the number of binding site (n) were calculated using Equation S3 and are listed in Table 3. The results show that the association constants K_A increased with the temperature, indicating the formation of stable adducts and endothermic processes; in addition, the values of n approximated to 1 suggest only one reactive site for both complexes in the protein. The interactions of HSA with **2b** and **2c** were relatively stronger than that with cisplatin; under the same conditions the binding constant Ka for cisplatin-HSA complex was of 8.52×10^2 M^{-1} [106]. Nevertheless, they were comparable to those obtained with ruthenium compounds and other platinum complexes (10^4–10^5 M^{-1}) [72,107–110].

Intermolecular interactions between a drug and a protein may involve van der Waals forces, hydrogen bonds, electrostatic forces and hydrophobic interactions [111]. To clarify the type of reaction between our complexes and HSA the thermodynamic parameters were calculated using the van't Hoff plots and Equations S4 and S5. Table 4 shows the values of ΔH^0 and ΔS^0 obtained from such relationships as well as the corresponding values for Gibbs free energy change (ΔG^0). The positive ΔH^0 and ΔS^0 for complexes **2b** and **2c** suggest that hydrophobic and ionic interactions might be involved. The negative values of ΔG^0 indicate that the interactions were spontaneous. The aromatic ring present in both complexes **2b** and **2c** enabled hydrophobic and π–π stacking interactions with amino acid residues in HSA such as Trp, Tyr and His; electrostatic interactions were also reasonable. It is known that cisplatin interacts with HSA generating irreversible covalent bonds but our compounds form reversible adducts via noncovalent interactions.

Table 3. The quenching and association parameters of the HSA-Pt systems at different temperatures.

T (K)	K_{SV} (M^{-1})		Kq ($M^{-1} \cdot s^{-1}$)		K_A (M^{-1})		*n*	
	2b	**2c**	**2b**	**2c**	**2b**	**2c**	**2b**	**2c**
300	8.85×10^3	1.36×10^4	1.77×10^{12}	2.72×10^{12}	9.88×10^3	1.45×10^4	1.26	1.25
305	9.78×10^3	1.48×10^4	1.96×10^{12}	2.96×10^{12}	9.90×10^3	1.52×10^4	0.96	0.99
310	1.04×10^4	1.62×10^4	2.08×10^{12}	3.24×10^{12}	1.10×10^4	1.59×10^4	1.24	1.59

Table 4. Thermodynamic parameters of the HSA-Pt systems at different temperatures.

T (K)	ΔH^0 (kJ mol^{-1})		ΔG^0 (kJ mol^{-1})		ΔS^0 (J $mol^{-1} \cdot K^{-1}$)	
	2b	**2c**	**2b**	**2c**	**2b**	**2c**
300	16.8	7.15	−22.7	−23.9	131.4	103.5
305			−23.3	−24.4		

Circular dichroism (CD) experiments were carried out to verify the binding of Pt(II) complexes to HSA and their effect on the protein secondary structure. The observed negative bands at wavelength of 208–209 and 222–223 nm (Figure S8) were characteristic of an α-helical structure of proteins. The binding of **2b** and **2c** to HSA reduced both bands. The θ values of the protein decreased with the increase in concentration of the platinum complexes with shifts in the bands positions indicating some loss of α-helical secondary structure. According to Equation (2) (see Experimental), the content of α-helix decreased from 50.88% to 46.29% and to 47.17% at an HSA/complex molar ratio of 1/10 for **2b** and **2c**, respectively. These changes indicate an interaction between our compounds and amino acid residues of the protein, which partially destroy existing hydrogen bonds. Nevertheless, the absence of changes in the shape of the spectra suggests the protein's secondary structure is still dominated by α-helix forms.

4. Conclusions

The new Pt(II) pentafluorophenyl complex ($PtCl(C_6F_5)(PTA)_2$) (**2a**) and its bis-cationic congeners with allyl-PTA(BF_4) (**2b**) and benzyl-PTA(BF_4) (**2c**) derivatives were synthesized and fully characterized by multinuclear NMR, ESI mass spectrometry and elemental analysis. All the complexes had a *trans* configuration of the aminophosphine ligands as confirmed by the PTA derivative X-ray structure obtained for the PTA derivative. Their biological activity was tested against NHDF, A549, HeLa and MCF7. The results have shown that **2a** and **2b** compounds had strong cytotoxicity against A549 and **2c** against HeLa cell lines. All three complexes showed lower cytotoxicity against fibroblasts cell line (NHDF). Cisplatin displayed the weakest cytotoxic activity against the chosen neoplastic cell lines (especially A549) in comparison to tested compounds. In addition, our compounds provided the great advantage of water solubility making this a positive feature against the frequently used DMSO. Complexes **2b** and **2c** interacted with human serum albumin causing a conformational change with the loss of helical stability of the protein. The binding affinity to HSA of the benzyl derivative **2c** was higher than that of the allyl **2a**. Concerning the thermodynamic parameters, the positive values of ΔH^0 and ΔS^0 and negative ΔG^0 for both complexes suggest that hydrophobic and ionic interactions participated in the interaction with HSA and the interaction of complexes with the protein was a spontaneous process. Further studies are necessary to assess the mechanism of action, to address the future synthetic efforts toward more active species.

Supplementary Materials: The following are available online at www.mdpi.com/xxx/s1, Figures S1–S5: ^{1}H NMR spectra of ligand **1b**, **1c**, **2a**, **2b** and **2c**, Figure S6: Stern-Volmer plots for quenching of HSA fluorescence by **2b** and **2c** at different concentrations and temperatures, Figure S7: Plots of $\log(F_0 - F)/F$ versus $\log(1/([Q] - (F_0 - F)[P_t]/F_0))$ at different temperatures for HSA in the presence of complexes **2b** and **2c,** Figure S8: Circular dichroism spectra of HSA in the absence and presence of platinum complexes **2b** and **2c**, Equations S1–S5.

Author Contributions: Investigation, P. Sgarbossa; Conceptualization and Formal analysis, P. Sgarbossa and P. Smoleński; X-ray analysis, M.F.C.G.d.S.; Biological analysis, U.Ś.-H., B.B., A.P., N.J., D.P.; Writing—original draft, P. Sgarbossa and P. Smoleński; Writing—review and editing, M.F.C.G.d.S., A.J.L.P., P. Sgarbossa and P. Smoleński; Supervision, M.F.C.G.d.S., P. Sgarbossa and P. Smoleński.

Funding: This research was funded by the Foundation for Science and Technology (FCT), project UID/QUI/00100/2019, Portugal, the NCN program (project 2012/07/B/ST/00885), Poland, and the AQUACHEM Network (HRTM project CMTN-CT-2003-503864). The coauthor is grateful to the Ministry of Science and Higher Education for support of this work (Grant No. Pbmn-48, Poland).

Acknowledgments: We wish to thank Dr. Tomasz Gębarowski (Department of Basic Medical Sciences, Faculty of Pharmacy with the Division of Laboratory Diagnostics, Wrocław Medical University, Poland) for providing cell lines.

Conflicts of Interest: The authors declare no conflict of interest.

References

1. Gonsalvi, L.; Guerriero, A.; Hapiot, F.; Krogstad, D.A.; Monflier, E.; Reginato, G.; Peruzzini, M. Lower-and Upper-Rim-Modified Derivatives of 1,3,5-Triaza-7-Phosphaadamantane: Coordination Chemistry and Applications in Catalytic Reactions in Water. *Pure Appl. Chem.* **2012**, *85*, 385–396.
2. Bravo, J.; Bolaño, S.; Gonsalvi, L.; Peruzzini, M. Coordination Chemistry of 1,3,5-Triaza-7-Phosphaadamantane (PTA) and Derivatives. Part II. The Quest for Tailored Ligands, Complexes and Related Applications. *Coord. Chem. Rev.* **2010**, *254*, 555–607.
3. Phillips, A.D.; Gonsalvi, L.; Romerosa, A.; Vizza, F.; Peruzzini, M. Coordination Chemistry of 1,3,5-Triaza-7-Phosphaadamantane (PTA): Transition Metal Complexes and Related Catalytic, Medicinal and Photoluminescent Applications. *Coord. Chem. Rev.* **2004**, *248*, 955–993.
4. Zatajska, A.; Siczek, M.; Skarżyńska, A.; Smoleński, P. New Water-Soluble Palladium(II) Iodide Complexes Derived from N-Protonated or N-Alkyl-1,3,5-Triaza-7-Phosphaadamantanes: Synthesis, Crystal Structure and Catalytic Properties in Aqua Media. *Inorg. Chim. Acta* **2017**, *455*, 701–706.
5. Mena-Cruz, A.; Serrano-Ruiz, M.; Lorenzo-Luis, P.; Romerosa, A.; Kathó, Á.; Joó, F.; Aguilera-Sáez, L.M. Evaluation of Catalytic Activity of $[RuClCp(Dmopta)(PPh_3)](OsO_2CF_3)$ in the Isomerization of Allylic

Alcohols in Water (Dmopta = 3, 7-Dimethyl-1,3,7-Triaza-5-Phosphabicyclo [3.3.1] Nonane). *J. Mol. Catal. A Chem.* **2016**, *411*, 27–33.

6. Chahdoura, F.; Favier, I.; Pradel, C.; Mallet-Ladeira, S.; Gómez, M. Palladium Nanoparticles Stabilised by PTA Derivatives in Glycerol: Synthesis and Catalysis in a Green Wet Phase. *Catal. Commun.* **2015**, *63*, 47–51.
7. Sears, J.M.; Lee, W.-C.; Frost, B.J. Water Soluble Diphosphine Ligands Based on 1,3,5-Triaza-7-Phosphaadamantane (PTA-Pr2): Synthesis, Coordination Chemistry, and Ruthenium Catalyzed Nitrile Hydration. *Inorg. Chim. Acta* **2015**, *431*, 248–257.
8. Bolyog-Nagy, E.; Udvardy, A.; Joó, F.; Kathó, Á. Efficient and Selective Hydration of Nitriles to Amides in Aqueous Systems with Ru(II)-Phosphaurotropine Catalysts. *Tetrahedron Lett.* **2014**, *55*, 3615–3617.
9. Sherbow, T.J.; Downs, E.L.; Sayler, R.I.; Razink, J.J.; Juliette, J.J.; Tyler, D.R. Investigation of 1,3,5-Triaza-7-Phosphaadamantane-Stabilized Silver Nanoparticles as Catalysts for the Hydration of Benzonitriles and Acetone Cyanohydrin. *ACS Catal.* **2014**, *4*, 3096–3104.
10. Serrano-Ruiz, M.; Lidrissi, C.; Mañas, S.; Peruzzini, M.; Romerosa, A. Synthesis, Reactivity and Catalytic Properties of the Allenylidene [Ru(Cccph$_2$)Cp(PTA)(Pph$_3$)](Cf$_3$SO$_3$) (PTA = 1,3,5-Triaza-7-Phosphaadamantane). *J. Organomet. Chem.* **2014**, *751*, 654–661.
11. Kapdi, A.; Gayakhe, V.; Sanghvi, Y.S.; Garcia, J.; Lozano, P.; da Silva, I.; Perez, J.; Serrano, J.L. New Water Soluble Pd-Imidate Complexes as Highly Efficient Catalysts for the Synthesis of C5-Arylated Pyrimidine Nucleosides. *RSC Adv.* **2014**, *4*, 17567–17572.
12. Lee, J.-Y.; Ghosh, D.; Lee, J.-Y.; Wu, S.-S.; Hu, C.-H.; Liu, S.-D.; Lee, H.M. Zwitterionic Palladium Complexes: Room-Temperature Suzuki–Miyaura Cross-Coupling of Sterically Hindered Substrates in an Aqueous Medium. *Organometallics* **2014**, *33*, 6481–6492.
13. Murray, B.S.; Babak, M.V.; Hartinger, C.G.; Dyson, P.J. The Development of RaPTA Compounds for the Treatment of Tumors. *Coord. Chem. Rev.* **2016**, *306*, 86–114.
14. Timerbaev, A.R. Role of Metallomic Strategies in Developing Ruthenium Anticancer Drugs. *TrAC Trends Anal. Chem.* **2016**, *80*, 547–554.
15. Daigle, D.J.; Decuir, T.J.; Robertson, J.B.; Darensbourg, D.J. 1,3,5-Triaz-7-Phosphatricyclo[3.3.1.1^{3,7}]Decane and Derivatives. *Inorg. Synth.* **1998**, *32*, 40–45.
16. Romerosa, A.; Campos-Malpartida, T.; Lidrissi, C.; Saoud, M.; Serrano-Ruiz, M.; Peruzzini, M.; Garrido-Cárdenas, J.A.; García-Maroto, F. Synthesis, Characterization, and DNA Binding of New Water-Soluble Cyclopentadienyl Ruthenium(II) Complexes Incorporating Phosphines. *Inorg. Chem.* **2006**, *45*, 1289–1298.
17. Wanke, R.; Smolenski, P.; Guedes da Silva, M.F.C.; Martins, L.M.; Pombeiro, A.J.L. Cu(I) Complexes Bearing the New Sterically Demanding and Coordination Flexible Tris(3-Phenyl-1-Pyrazolyl)Methanesulfonate Ligand and the Water-Soluble Phosphine 1,3,5-Triaza-7-Phosphaadamantane or Related Ligands. *Inorg. Chem.* **2008**, *47*, 10158–10168.
18. Pruchnik, F.P.; Smoleński, P. New Rhodium(I) Water-Soluble Complexes with 1-Alkyl-1-Azonia-3, 5-Diaza-7-Phospha-Adamantane Iodides and Their Catalytic Activity. *Appl. Organomet. Chem.* **1999**, *13*, 829–836.
19. Forward, J.; Staples, R.; Liu, C.; Fackler, J. Luminescent Tris (3-Ethyl-1, 5-Diaza-3-Azonia-7-Phosphatricyclo [3.3.1.1^{3,7}] Decane-P) Gold(I) Tetraiodide Trihydrate,[(Ettpa) 3Au]I4.3h2o. *Acta Crystallogr. Sect. C Cryst. Struct. Commun.* **1997**, *53*, 195–197.
20. Kirillov, A.M.; Smolenski, P.; Ma, Z.; Guedes da Silva, M.F.C.; Haukka, M.; Pombeiro, A.J.L. Copper(I) Iodide Complexes Derived from N-Alkyl-1,3,5-Triaza-7-Phosphaadamantanes: Synthesis, Crystal Structures, Photoluminescence, and Identification of the Unprecedented {Cu$_3$I$_5$}2—Cluster. *Organometallics* **2009**, *28*, 6425–6431.
21. Kirillov, A.M.; Smolenski, P.; Haukka, M.; Guedes da Silva, M.F.C.; Pombeiro, A.J.L. Unprecedented Metal-Free C(Sp3)–C(Sp3) Bond Cleavage: Switching from N-Alkyl-to N-Methyl-1,3,5-Triaza-7-Phosphaadamantane. *Organometallics* **2009**, *28*, 1683–1687.
22. Bergamini, P.; Marvelli, L.; Marchi, A.; Vassanelli, F.; Fogagnolo, M.; Formaglio, P.; Bernardi, T.; Gavioli, R.; Sforza, F. Platinum and Ruthenium Complexes of New Long-Tail Derivatives of PTA (1,3,5-Triaza-7-Phosphaadamantane): Synthesis, Characterization and Antiproliferative Activity on Human Tumoral Cell Lines. *Inorg. Chim. Acta* **2012**, *391*, 162–170.

23. Legrand, F.-X.; Hapiot, F.; Tilloy, S.; Guerriero, A.; Peruzzini, M.; Gonsalvi, L.; Monflier, E. Aqueous Rhodium-Catalyzed Hydroformylation of 1-Decene in the Presence of Randomly Methylated B-Cyclodextrin and 1,3,5-Triaza-7-Phosphaadamantane Derivatives. *Appl. Catal. A Gen.* **2009**, *362*, 62–66.
24. Fluck, E.; Förster, J.-E.; Weidlein, J.; Hädicke, E. 1.3. 5-Triaza-7-Phosphaadamantan (Monophospha-Urotropin)/1,3,5-Triaza-7-Phosphaadamantane (Monophospha-Urotropine). *Zeitschrift für Naturforschung B* **1977**, *32*, 499–506.
25. Smoleński, P.; Kirillov, A.M.; Guedes da Silva, M.F.C.; Pombeiro, A.J.L. 1-Methyl-1-Azonia-3, 5-Diaza-7-Phosphatricyclo [3.3.1.1^{3,7}] Decane Tetrafluoroborate. *Acta Crystallogr. Sect. E Struct. Rep. Online* **2008**, *64*, o556.
26. Krogstad, D.A.; Ellis, G.S.; Gunderson, A.K.; Hammrich, A.J.; Rudolf, J.W.; Halfen, J.A. Two New Water-Soluble Derivatives of 1,3,5-Triaza-7-Phosphaadamantane (PTA): Synthesis, Characterization, X-Ray Analysis and Solubility Studies of 3,7-Diformyl-1,3,7-Triaza-5-Phosphabicyclo [3.3.1] Nonane and 1-Pyridylmethyl-3,5-Diaza-1-Azonia-7-Phosphatricyclo [3.3.1.1] Decane Bromide. *Polyhedron* **2007**, *26*, 4093–4100.
27. Singh, K.; Jana, A.; Lippmann, P.; Ott, I.; Das, N. Isomeric Platinum Organometallics Derived from Pyrimidine, Pyridazine or Pyrazine and Their Potential as Antitumor Drugs. *Inorg. Chim. Acta* **2019**, *493*, 112–117.
28. Cullinane, C.; Deacon, G.B.; Drago, P.R.; Erven, A.P.; Junk, P.C.; Luu, J.; Meyer, G.; Schmitz, S.; Ott, I.; Schur, J. Synthesis and Antiproliferative Activity of a Series of New Platinum and Palladium Diphosphane Complexes. *Dalton Trans.* **2018**, *47*, 1918–1932.
29. Medrano, M.Á.; Álvarez-Valdés, A.; Perles, J.; Lloret-Fillol, J.; Muñoz-Galván, S.; Carnero, A.; Navarro-Ranninger, C.; Quiroga, A.G. Oxidation of Anticancer Pt(II) Complexes with Monodentate Phosphane Ligands: Towards Stable but Active Pt(Iv) Prodrugs. *Chem. Commun.* **2013**, *49*, 4806–4808.
30. Ramos-Lima, F.J.; Quiroga, A.G.; García-Serrelde, B.; Blanco, F.; Carnero, A.; Navarro-Ranninger, C. New Trans-Platinum Drugs with Phosphines and Amines as Carrier Ligands Induce Apoptosis in Tumor Cells Resistant to Cisplatin. *J. Med. Chem.* **2007**, *50*, 2194–2199.
31. Ramos-Lima, F.J.; Quiroga, A.G.; Pérez, J.M.; Font-Bardía, M.; Solans, X.; Navarro-Ranninger, C. Synthesis and Characterization of New Transplatinum Complexes Containing Phosphane Groups-Cytotoxic Studies in Cisplatin-Resistant Cells. *Eur. J. Inorg. Chem.* **2003**, *2003*, 1591–1598.
32. Neplechová, K.; Kašpárková, J.; Vrána, O.; Nováková, O.; Habtemariam, A.; Watchman, B.; Sadler, P.J.; Brabec, V. DNA Interactions of New Antitumor Aminophosphine Platinum(II) Complexes. *Mol. Pharmacol.* **1999**, *56*, 20–30.
33. Živković, M.; Kljun, J.; Ilic-Tomic, T.; Pavic, A.; Veselinović, A.; Manojlović, D.D.; Nikodinovic-Runic, J.; Turel, I. A New Class of Platinum(II) Complexes with the Phosphine Ligand PTA Which Show Potent Anticancer Activity. *Inorg. Chem. Front.* **2018**, *5*, 39–53.
34. Cortesi, R.; Damiani, C.; Ravani, L.; Marvelli, L.; Esposito, E.; Drechsler, M.; Pagnoni, A.; Mariani, P.; Sforza, F.; Bergamini, P. Lipid-Based Nanoparticles Containing Cationic Derivatives of PTA (1,3,5-Triaza-7-Phosphaadamantane) as Innovative Vehicle for Pt Complexes: Production, Characterization and in Vitro Studies. *Int. J. Pharm.* **2015**, *492*, 291–300.
35. Mügge, C.; Rothenburger, C.; Beyer, A.; Görls, H.; Gabbiani, C.; Casini, A.; Michelucci, E.; Landini, I.; Nobili, S.; Mini, E. Structure, Solution Chemistry, Antiproliferative Actions and Protein Binding Properties of Non-Conventional Platinum(II) Compounds with Sulfur and Phosphorus Donors. *Dalton Trans.* **2011**, *40*, 2006–2016.
36. Bergamini, P.; Bertolasi, V.; Marvelli, L.; Canella, A.; Gavioli, R.; Mantovani, N.; Manas, S.; Romerosa, A. Phosphinic Platinum Complexes with 8-Thiotheophylline Derivatives: Synthesis, Characterization, and Antiproliferative Activity. *Inorg. Chem.* **2007**, *46*, 4267–4276.
37. Romerosa, A.; Bergamini, P.; Bertolasi, V.; Canella, A.; Cattabriga, M.; Gavioli, R.; Mañas, S.; Mantovani, N.; Pellacani, L. Biologically Active Platinum Complexes Containing 8-Thiotheophylline and 8-(Methylthio) Theophylline. *Inorg. Chem.* **2004**, *43*, 905–913.
38. Sánchez-de-Diego, C.; Mármol, I.; Pérez, R.; Gascón, S.; Rodriguez-Yoldi, M.J.; Cerrada, E. The Anticancer Effect Related to Disturbances in Redox Balance on Caco-2 Cells Caused by an Alkynyl Gold(I) Complex. *J. Inorg. Biochem.* **2017**, *166*, 108–121.

39. Atrián-Blasco, E.; Gascón, S.; Rodríguez-Yoldi, M.J.; Laguna, M.; Cerrada, E. Synthesis of Gold(I) Derivatives Bearing Alkylated 1,3,5-Triaza-7-Phosphaadamantane as Selective Anticancer Metallodrugs. *Eur. J. Inorg. Chem.* **2016**, *2016*, 2791–2803.
40. García-Moreno, E.; Tomás, A.; Atrián-Blasco, E.; Gascón, S.; Romanos, E.; Rodriguez-Yoldi, M.J.; Cerrada, E.; Laguna, M. In Vitro and in Vivo Evaluation of Organometallic Gold(I) Derivatives as Anticancer Agents. *Dalton Trans.* **2016**, *45*, 2462–2475.
41. Pettinari, R.; Condello, F.; Marchetti, F.; Pettinari, C.; Smoleński, P.; Riedel, T.; Scopelliti, R.; Dyson, P.J. Dicationic Ruthenium(II)-Arene-Curcumin Complexes Containing Methylated 1,3,5-Triaza-7-Phosphaadamantane: Synthesis, Structure, and Cytotoxicity. *Eur. J. Inorg. Chem.* **2017**, *2017*, 2905–2910.
42. Pettinari, R.; Petrini, A.; Marchetti, F.; Pettinari, C.; Riedel, T.; Therrien, B.; Dyson, P.J. Arene-Ruthenium(II) Complexes with Bioactive Ortho-Hydroxydibenzoylmethane Ligands: Synthesis, Structure, and Cytotoxicity. *Eur. J. Inorg. Chem.* **2017**, *2017*, 1800–1806.
43. Berndsen, R.H.; Weiss, A.; Abdul, U.K.; Wong, T.J.; Meraldi, P.; Griffioen, A.W.; Dyson, P.J.; Nowak-Sliwinska, P. Combination of Ruthenium(II)-Arene Complex [Ru(H 6-P-Cymene)Cl2(PTA)](RaPTA-C) and the Epidermal Growth Factor Receptor Inhibitor Erlotinib Results in Efficient Angiostatic and Antitumor Activity. *Sci. Rep.* **2017**, *7*, 43005.
44. Battistin, F.; Scaletti, F.; Balducci, G.; Pillozzi, S.; Arcangeli, A.; Messori, L.; Alessio, E. Water-Soluble Ru(II)- and Ru(III)-Halide-PTA Complexes (PTA = 1,3,5-Triaza-7-Phosphaadamantane): Chemical and Biological Properties. *J. Inorg. Biochem.* **2016**, *160*, 180–188.
45. Guidi, F.; Modesti, A.; Landini, I.; Nobili, S.; Mini, E.; Bini, L.; Puglia, M.; Casini, A.; Dyson, P.J.; Gabbiani, C. The Molecular Mechanisms of Antimetastatic Ruthenium Compounds Explored through Dige Proteomics. *J. Inorg. Biochem.* **2013**, *118*, 94–99.
46. Pettinari, R.; Marchetti, F.; Petrini, A.; Pettinari, C.; Lupidi, G.; Smoleński, P.; Scopelliti, R.; Riedel, T.; Dyson, P.J. From Sunscreen to Anticancer Agent: Ruthenium(II) Arene Avobenzone Complexes Display Potent Anticancer Activity. *Organometallics* **2016**, *35*, 3734–3742.
47. Wołoszyn, A.; Pettinari, C.; Pettinari, R.; Patzmay, G.V.B.; Kwiecień, A.; Lupidi, G.; Nabissi, M.; Santoni, G.; Smoleński, P. Ru(II)-(PTA) and -MPTA Complexes with N 2-Donor Ligands Bipyridyl and Phenanthroline and Their Antiproliferative Activities on Human Multiple Myeloma Cell Lines. *Dalton Trans.* **2017**, *46*, 10073–10081.
48. Tapanelli, S.; Habluetzel, A.; Pellei, M.; Marchiò, L.; Tombesi, A.; Capparè, A.; Santini, C. Novel Metalloantimalarials: Transmission Blocking Effects of Water Soluble Cu(I), Ag(I) and Au(I) Phosphane Complexes on the Murine Malaria Parasite Plasmodium Berghei. *J. Inorg. Biochem.* **2017**, *166*, 1–4.
49. Jaros, S.W.; Guedes da Silva, M.F.C.; Florek, M.; Smoleński, P.; Pombeiro, A.J.L.; Kirillov, A.M. Silver(I) 1,3,5-Triaza-7-Phosphaadamantane Coordination Polymers Driven by Substituted Glutarate and Malonate Building Blocks: Self-Assembly Synthesis, Structural Features, and Antimicrobial Properties. *Inorg. Chem.* **2016**, *55*, 5886–5894.
50. Smolenski, P.; Pettinari, C.; Marchetti, F.; Guedes da Silva, M.F.C.; Lupidi, G.; Badillo Patzmay, G.V.; Petrelli, D.; Vitali, L.A.; Pombeiro, A.J.L. Syntheses, Structures, and Antimicrobial Activity of New Remarkably Light-Stable and Water-Soluble Tris (Pyrazolyl) Methanesulfonate Silver(I) Derivatives of N-Methyl-1,3,5-Triaza-7-Phosphaadamantane Salt-[MPTA] Bf4. *Inorg. Chem.* **2014**, *54*, 434–440.
51. Jaros, S.W.; Guedes da Silva, M.F.C.; Król, J.; Conceição Oliveira, M.; Smoleński, P.; Pombeiro, A.J.L.; Kirillov, A.M. Bioactive Silver-Organic Networks Assembled from 1,3,5-Triaza-7-Phosphaadamantane and Flexible Cyclohexanecarboxylate Blocks. *Inorg. Chem.* **2016**, *55*, 1486–1496.
52. Gandin, V.; Trenti, A.; Porchia, M.; Tisato, F.; Giorgetti, M.; Zanusso, I.; Trevisi, L.; Marzano, C. Homoleptic Phosphino Copper(I) Complexes with in Vitro and in Vivo Dual Cytotoxic and Anti-Angiogenic Activity. *Metallomics* **2015**, *7*, 1497–1507.
53. Gandin, V.; Tisato, F.; Dolmella, A.; Pellei, M.; Santini, C.; Giorgetti, M.; Marzano, C.; Porchia, M. In Vitro and in Vivo Anticancer Activity of Copper(I) Complexes with Homoscorpionate Tridentate Tris(Pyrazolyl)Borate and Auxiliary Monodentate Phosphine Ligands. *J. Med. Chem.* **2014**, *57*, 4745–4760.
54. García-Moreno, E.; Gascón, S.; Rodriguez-Yoldi, M.J.; Cerrada, E.; Laguna, M. S-Propargylthiopyridine Phosphane Derivatives as Anticancer Agents: Characterization and Antitumor Activity. *Organometallics* **2013**, *32*, 3710–3720.

55. Santini, C.; Pellei, M.; Papini, G.; Morresi, B.; Galassi, R.; Ricci, S.; Tisato, F.; Porchia, M.; Rigobello, M.P.; Gandin, V. In Vitro Antitumour Activity of Water Soluble Cu(I), Ag(I) and Au(I) Complexes Supported by Hydrophilic Alkyl Phosphine Ligands. *J. Inorg. Biochem.* **2011**, *105*, 232–240.
56. Lipfert, J.; Doniach, S.; Das, R.; Herschlag, D. Understanding Nucleic Acid-Ion Interactions. *Annu. Rev. Biochem.* **2014**, *83*, 813–841.
57. Riddell, I.A.; Johnstone, T.C.; Park, G.Y.; Lippard, S.J. Nucleotide Binding Preference of the Monofunctional Platinum Anticancer-Agent Phenanthriplatin. *Chemistry* **2016**, *22*, 7574–7581.
58. Amir, M.K.; Hayat, F.; Khan, S.Z.; Hogarth, G.; Kondratyuk, T.; Pezzuto, J.M.; Tahir, M.N. Monofunctional Platinum(II) Dithiocarbamate Complexes: Synthesis, Characterization and Anticancer Activity. *RSC Adv.* **2016**, *6*, 110517–110524.
59. Villarreal, W.; Colina-Vegas, L.; Rodrigues de Oliveira, C.; Tenorio, J.C.; Ellena, J.; Gozzo, F.C.; Cominetti, M.R.; Ferreira, A.G.; Ferreira, M.A.B.; Navarro, M. Chiral Platinum(II) Complexes Featuring Phosphine and Chloroquine Ligands as Cytotoxic and Monofunctional DNA-Binding Agents. *Inorg. Chem.* **2015**, *54*, 11709–11720.
60. Cutillas, N.; Martínez, A.; Yellol, G.S.; Rodríguez, V.; Zamora, A.; Pedreño, M.; Donaire, A.; Janiak, C.; Ruiz, J. Anticancer C, N-Cycloplatinated(II) Complexes Containing Fluorinated Phosphine Ligands: Synthesis, Structural Characterization, and Biological Activity. *Inorg. Chem.* **2013**, *52*, 13529–13535.
61. Berenguer, J.; Pichel, J.; Gimenez, N.; Lalinde, E.; Moreno, M.; Pineiro-Hermida, S. Luminescent Pentafluorophenyl-Cycloplatinated Complexes: Synthesis, Characterization, Photophysics, Cytotoxicity and Cellular Imaging. *Dalton Trans.* **2015**, *44*, 18839–18855.
62. Cullinane, C.; Deacon, G.B.; Drago, P.R.; Hambley, T.W.; Nelson, K.T.; Webster, L.K. Preparation and Cell Growth Inhibitory Activity of $[PtR_2L_2]$(R = Polyfluorophenyl, L_2= Diene, Cyclohexane-1, 2-Diamine (Chxn) or Cis-(Dimethyl Sulfoxide)2) and the X-Ray Crystal Structure of $[Pt(C_6F_5)_2$(Cis-Chxn)]. *J. Inorg. Biochem.* **2002**, *89*, 293–301.
63. Minniti, D. Uncatalyzed Cis-Trans Isomerization of Bis(Pentafluorophenyl) Bis(Tetrahydrothiophene) Palladium(II) Complexes in Chloroform: Evidence for a Dissociative Mechanism. *Inorg. Chem.* **1994**, *33*, 2631–2634.
64. García-Monforte, M.A.; Alonso, P.J.; Forniés, J.; Menjón, B. New Advances in Homoleptic Organotransition-Metal Compounds: The Case of Perhalophenyl Ligands. *Dalton Trans.* **2007**, *38*, 3347–3359.
65. Pizzo, E.; Sgarbossa, P.; Scarso, A.; Michelin, R.A.; Strukul, G. Second-Generation Electron-Poor Platinum(II) Complexes as Efficient Epoxidation Catalysts for Terminal Alkenes with Hydrogen Peroxide. *Organometallics* **2006**, *25*, 3056–3062.
66. Stone, F.G.A. Fluorocarbon Metal Compounds—Role Models in Organotransition Metal Chemistry. *J. Fluor. Chem.* **1999**, *100*, 227–234.
67. Usón, R.; Forniés, J. Organopalladium and Platinum Compounds with Pentahalophenyl Ligands. *Adv. Organomet. Chem.* **1988**, *28*, 219–297.
68. Sarkar, B. Metal Protein Interactions. *Prog. Food Nutr. Sci.* **1987**, *11*, 363–400.
69. Bal, W.; Christodoulou, J.; Sadler, P.J.; Tucker, A. Multi-Metal Binding Site of Serum Albumin. *J. Inorg. Biochem.* **1998**, *70*, 33–39.
70. Espósito, B.P.; Najjar, R. Interactions of Antitumoral Platinum-Group Metallodrugs with Albumin. *Coord. Chem. Rev.* **2002**, *232*, 137–149.
71. Hu, W.; Luo, Q.; Wu, K.; Li, X.; Wang, F.; Chen, Y.; Ma, X.; Wang, J.; Liu, J.; Xiong, S. The Anticancer Drug Cisplatin Can Cross-Link the Interdomain Zinc Site on Human Albumin. *Chem. Commun.* **2011**, *47*, 6006–6008.
72. Zheng, Y.-R.; Suntharalingam, K.; Johnstone, T.C.; Yoo, H.; Lin, W.; Brooks, J.G.; Lippard, S.J. Pt(IV) Prodrugs Designed to Bind Non-Covalently to Human Serum Albumin for Drug Delivery. *J. Am. Chem. Soc.* **2014**, *136*, 8790–8798.
73. Ivanov, A.I.; Christodoulou, J.; Parkinson, J.A.; Barnham, K.J.; Tucker, A.; Woodrow, J.; Sadler, P.J. Cisplatin Binding Sites on Human Albumin. *J. Biol. Chem.* **1998**, *273*, 14721–14730.
74. Guerrero, E.; Miranda, S.; Lüttenberg, S.; Fröhlich, N.; Koenen, J.-M.; Mohr, F.; Cerrada, E.; Laguna, M.; Mendía, A. Trans-Thionate Derivatives of Pt(II) and Pd(II) with Water-Soluble Phosphane PTA and DAPTA Ligands: Antiproliferative Activity against Human Ovarian Cancer Cell Lines. *Inorg. Chem.* **2013**, *52*, 6635–6647.

75. Dalla Via, L.; García-Argáez, A.N.; Agostinelli, E.; Dell'Amico, D.B.; Labella, L.; Samaritani, S. New Trans Dichloro(Triphenylphosphine)Platinum(II) Complexes Containing N-(Butyl), N-(Arylmethyl)Amino Ligands: Synthesis, Cytotoxicity and Mechanism of Action. *Biorg. Med. Chem.* **2016**, *24*, 2929–2937.
76. Quiroga, A. Understanding Trans Platinum Complexes as Potential Antitumor Drugs Beyond Targeting DNA. *J. Inorg. Biochem.* **2012**, *114*, 106–112.
77. Kalinowska-Lis, U.; Ochocki, J.; Matlawska-Wasowska, K. Trans Geometry in Platinum Antitumor Complexes. *Coord. Chem. Rev.* **2008**, *252*, 1328–1345.
78. Yilmaz, V.T.; Icsel, C.; Turgut, O.R.; Aygun, M.; Erkisa, M.; Turkdemir, M.H.; Ulukaya, E. Synthesis, Structures and Anticancer Potentials of Platinum(II) Saccharinate Complexes of Tertiary Phosphines with Phenyl and Cyclohexyl Groups Targeting Mitochondria and DNA. *Eur. J. Med. Chem.* **2018**, *155*, 609–622.
79. Echeverri, M.; Alvarez-Valdés, A.; Navas, F.; Perles, J.; Sánchez-Pérez, I.; Quiroga, A.G. Using Phosphine Ligands with a Biological Role to Modulate Reactivity in Novel Platinum Complexes. *R. Soc. Open Sci.* **2018**, *5*, 171340.
80. Armarego, W.L. *Purification of Laboratory Chemicals*; Butterworth-Heinemann: Oxford, UK, 2017.
81. Usón, R.; Forniés, J.; Espinet, P.; Alfranca, G. Pentafluorophenyl Platinum(II) and Platinum(IV) Complexes with O-Phenylenebisdimethylarsine. *Synth. React. Inorg. Met. Org. Chem.* **1980**, *10*, 579–590.
82. Usón, R.; Forniés, J.; Martínez, F.; Tomás, M. Mono- and Bi-Nuclear Anionic Pentafluorophenyl Complexes of Palladium(II) and Platinum(II). *J. Chem. Soc. Dalton Trans.* **1980**, 888–894. doi:10.1039/DT9800000888.
83. *EN 14476. Chemical Disinfectants and Antiseptics—Quantitative Suspension Test for the Evaluation of Virucidal Activity in the Medical Area—Test Method and Requirements (Phase 2/Step 1)*. NSAI: Dublin, Ireland, 2015.
84. Sangster, J. Octanol-Water Partition Coefficients of Simple Organic Compounds. *J. Phys. Chem. Ref. Data* **1989**, *18*, 1111–1229.
85. Beaven, G.H.; Chen, S.H.; D'albis, A.; Gratzer, W.B. A Spectroscopic Study of the Haemin-Human-Serum-Albumin System. *Eur. J. Biochem.* **1974**, *41*, 539–546.
86. Kumaran, R.; Ramamurthy, P. Photophysical Studies on the Interaction of Amides with Bovine Serum Albumin (BSA) in Aqueous Solution: Fluorescence Quenching and Protein Unfolding. *J. Lumin.* **2014**, *148*, 277–284.
87. Bruker. *APEX2*; Bruker AXS Inc.: Madison, WI, USA, 2012.
88. Sheldrick, G.M. *SADABS. Program for Empirical Absorption Correction*; University of Gottingen: Gottingen, Germany, 1996.
89. Altomare, A.; Burla, M.C.; Camalli, M.; Cascarano, G.L.; Giacovazzo, C.; Guagliardi, A.; Moliterni, A.G.; Polidori, G.; Spagna, R. Sir97: A New Tool for Crystal Structure Determination and Refinement. *J. Appl. Crystallogr.* **1999**, *32*, 115–119.
90. Sheldrick, G.M. A Short History of Shelx. *Acta Crystallogr. Sect. A Found. Crystallogr.* **2008**, *64*, 112–122.
91. Farrugia, L.J. Wingx and Ortep for Windows: An Update. *J. Appl. Crystallogr.* **2012**, *45*, 849–854.
92. Smoleński, P.; Pombeiro, A.J.L. Water-Soluble and Stable Dinitrogen Phosphine Complexes Trans-[Recl(N_2)(PTA-H)N(PTA)$_4$–N]N+ (N = 0–4), the First with 1,3,5-Triaza-7-Phosphaadamantane. *Dalton Trans.* **2008**, 87–91. doi:10.1039/b712360d.
93. Yang, L.; Powell, D.R.; Houser, R.P. Structural Variation in Copper(I) Complexes with Pyridylmethylamide Ligands: Structural Analysis with a New Four-Coordinate Geometry Index, T 4. *Dalton Trans.* **2007**, *9*, 955–964.
94. Longmire, J.M.; Zhang, X.; Shang, M. Synthesis and X-Ray Crystal Structures of Palladium(II) and Platinum(II) Complexes of the Pcp-Type Chiral Tridentate Ligand (1R,1′R)-1,3-Bis[1-(Diphenylphosphino)Ethyl]Benzene. Use in the Asymmetric Aldol Reaction of Methyl Isocyanoacetate and Aldehydes. *Organometallics* **1998**, *17*, 4374–4379.
95. Lasri, J.; Guedes da Silva, M.F.C.; Kopylovich, M.N.; Ghosh Mukhopadhyay, B.; Pombeiro, A.J.L. Platinum(II)-Promoted [2 + 3] Cycloaddition of Azide with 4-Cyanobenzaldehyde, a Schiff Base Derivative or Dicyanobenzenes to Give Formyl-, Amino (Imino)-or Cyano-Functionalized Tetrazolato Complexes. *Eur. J. Inorg. Chem.* **2009**, *2009*, 5541–5549.
96. Smoleński, P.; Mukhopadhyay, S.; Guedes da Silva, M.F.C.; Charmier, M.A.J.; Pombeiro, A.J.L. New Water-Soluble Azido-and Derived Tetrazolato-Platinum(II) Complexes with PTA. Easy Metal-Mediated Synthesis and Isolation of 5-Substituted Tetrazoles. *Dalton Trans.* **2008**, 6546–6555. doi:10.1039/b808156e.

97. Sgarbossa, P.; Guedes da Silva, M.F.C.; Scarso, A.; Michelin, R.A.; Pombeiro, A.J.L. Lewis Acidity of Platinum(II)-Based Baeyer—Villiger Catalysts: An Electrochemical Approach. *Inorg. Chim. Acta* **2008**, *361*, 3247–3253.
98. Mukhopadhyay, S.; Lasri, J.; Guedes da Silva, M.F.C.; Charmier, M.A.J.; Pombeiro, A.J.L. Activation of C–Cn Bond of Propionitrile: An Alternative Route to the Syntheses of 5-Substituted-1h-Tetrazoles and Dicyano-Platinum(II) Species. *Polyhedron* **2008**, *27*, 2883–2888.
99. Lasri, J.; Charmier, M.A.J.; Guedes da Silva, M.F.C.; Pombeiro, A.J.L. Mixed Unsymmetric Oxadiazoline and/or Imine Platinum(II) Complexes. *Dalton Trans.* **2007**, 3259–3266. doi:10.1039/B704329E.
100. Jaros, S.W.; Śliwińska-Hill, U.; Białońska, A.; Nesterov, D.S.; Kuropka, P.; Sokolnicki, J.; Bażanów, B.; Smoleński, P. Light-Stable Polypyridine Silver(I) Complexes of 1,3,5-Triaza-7-Phosphaadamantane (PTA) and 1,3,5-Triaza-7-Phosphaadamantane-7-Sulfide (PTA = S): Significant Antiproliferative Activity of Representative Examples in Aqueous Media. *Dalton Trans.* **2019**, *48*, 11235–11249.
101. Wilson, J.J.; Lippard, S.J. In Vitro Anticancer Activity of Cis-Diammineplatinum(II) Complexes with B-Diketonate Leaving Group Ligands. *J. Med. Chem.* **2012**, *55*, 5326–5336.
102. Lakowicz, J.R. *Principles of Fluorescence Spectroscopy*, 3rd ed.; Springer: New York, NY, USA, 2006.
103. Klajnert, B.; Bryszewska, M. Fluorescence Studies on Pamam Dendrimers Interactions with Bovine Serum Albumin. *Bioelectrochemistry* **2002**, *55*, 33–35.
104. Ware, W.R. Oxygen Quenching of Fluorescence in Solution: An Experimental Study of the Diffusion Process. *J. Phys. Chem.* **1962**, *66*, 455–458.
105. Seedher, N.; Kanojia, M. Fluorescence Spectroscopic Studies on the Complexation of Antidiabetic Drugs with Glycosylated Serum Albumin. *J. Appl. Spectrosc.* **2013**, *80*, 754–760.
106. Neault, J.; Tajmir-Riahi, H. Interaction of Cisplatin with Human Serum Albumin. Drug Binding Mode and Protein Secondary Structure. *Biochim. Biophys. Acta* **1998**, *1384*, 153–159.
107. Morais, T.S.; Santos, F.C.; Corte-Real, L.; Garcia, M.H. Exploring the Effect of the Ligand Design on the Interactions between [Ru(η5 -C5h5)(Pph3)(N, O)][Cf3SO3] Complexes and Human Serum Albumin. *J. Inorg. Biochem.* **2013**, *129*, 94–101.
108. Liu, Y.; Yu, Q.; Wang, C.; Sun, D.; Huang, Y.; Zhou, Y.; Liu, J. Ruthenium(II) Complexes Binding to Human Serum Albumin and Inducing Apoptosis of Tumor Cells. *Inorg. Chem. Commun.* **2012**, *24*, 104–109.
109. Wang, Y.; Wang, X.; Wang, J.; Zhao, Y.; He, W.; Guo, Z. Noncovalent Interactions between a Trinuclear Monofunctional Platinum Complex and Human Serum Albumin. *Inorg. Chem.* **2011**, *50*, 12661–12668.
110. Krause-Heuer, A.M.; Price, W.S.; Aldrich-Wright, J.R. Spectroscopic Investigations on the Interactions of Potent Platinum(II) Anticancer Agents with Bovine Serum Albumin. *J. Chem. Biol.* **2012**, *5*, 105–113.
111. Leckband, D. Measuring the Forces That Control Protein Interactions. *Annu. Rev. Biophys. Biomol. Struct.* **2000**, *29*, 1–26.